

## Configurational Characteristics of Poly(methyl methacrylate)

P. R. Sundararajan and P. J. Flory\*

Contribution from the Department of Chemistry, Stanford University, Stanford, California 94305. Received February 12, 1974

**Abstract:** Poly(methyl methacrylate) is an example of a disubstituted vinyl chain in which the substituents COOCH<sub>3</sub> and CH<sub>3</sub> differ in size and shape; the former is noncylindrical, and the latter resembles the CH<sub>2</sub> skeletal group in its steric interactions. Owing to the planarity of the ester group, severe steric overlaps involving one or the other of its O atoms occur in the  $\bar{g}$  conformation of a skeletal bond irrespective of the rotational states of neighboring bonds. Conformational energy calculations indicate the  $\bar{g}$  state to be at least 7 kcal mol<sup>-1</sup> higher than the  $t$  and the  $g$  states. With the exclusion of the former conformation, all interactions of long range are eliminated, and the statistical weight matrices  $U'$  and  $U''$  for the respective skeletal bond pairs reduce to  $2 \times 2$  order. The contour energy surface computed as a function of bond rotations  $\varphi_i$  and  $\varphi_{i+1}$  within a dyad shows pairs of minima displaced *ca.*  $\pm 15^\circ$ ,  $\mp 15^\circ$  from the staggered conformations. Inasmuch as these displacements are small and symmetric, it is legitimate to treat each such pair of minima as a single state. Conformational energies and statistical weights accordingly were averaged over the region of each such state. Agreement with the experimental values of the characteristic ratio  $C_\infty = \langle (r^2)_0/nl^2 \rangle_\infty = 9.2$ – $10.7$  for isotactic PMMA and 7.3–8.4 for syndiotactic PMMA is obtained by taking  $E_\alpha \approx 1.1$  kcal mol<sup>-1</sup> and  $E_\beta \approx -0.6$  kcal mol<sup>-1</sup>,  $\alpha$  and  $\beta$  being the statistical weights for the meso,  $gt$  and the racemic,  $tt$  states, respectively, relative to the meso,  $tt$  state. The temperature coefficient  $d(\ln C_\infty)/dT$  calculated using these energies is negative for isotactic PMMA; it is positive for syndiotactic PMMA. These predictions appear to be supported by the limited experimental results that are available.

The poly(methyl methacrylate) (PMMA) chain bears two different substituents,  $R = \text{COOCH}_3$  and  $R' = \text{CH}_3$ , the latter of which resembles methylene (CH<sub>2</sub>) in its effective size. This in conjunction with the further fact that substituents  $R$  and  $R'$  differ suggests it as an example of case *i* of the preceding paper (I).<sup>1</sup> However, PMMA departs from case *i* in that the substituent  $R = \text{COOCH}_3$  is not cylindrically symmetric. Careful examination of models reveals this feature to be of major importance; an entire class of conformations  $\bar{g}$  is virtually suppressed on this account, as we show below.

In order to clarify the character of various interactions in the PMMA chain, we have carried out conformational energy calculations using conventional empirical methods. In recognition of the limitations of these methods, we rely on them principally to delineate the locations of accessible regions of conformational space. Allowances for inaccuracies in estimated energies are taken into account in the calculations of the mean-square end-to-end distance and its temperature coefficient.

## Conformational Energies

**Parameters for the Energy Calculations.** Three-fold intrinsic torsional potentials with barriers of 2.8 and 1.0 kcal mol<sup>-1</sup> were assigned to rotations around the skeletal C–C bonds and the C<sup>α</sup>–C\* bonds, respectively (see Figure 1). Nonbonded interactions were computed using the Lennard-Jones function  $E_{ij} = (a_{ij}/r_{ij}^{12}) - (b_{ij}/r_{ij}^6)$  for each pair of interacting atoms or groups.<sup>2–4</sup> The constant  $b_{ij}$  governing dispersion interactions was evaluated according to the Slater–Kirkwood formula from atom or group polarizabilities  $\alpha_i$  and the effective numbers of electrons  $N_i$ . The values of these

parameters used in the present calculations are given in Table I together with the adjusted<sup>3,4</sup> van der Waals

**Table I.** Parameters Used for Evaluating the Nonbonded Interaction Energy

Atom or group	van der Waals radius, Å	Effective no. of electrons, $N_i$	Polarizability $\alpha_i$ , Å <sup>3</sup>
C(carbonyl)	1.8	5	1.23
C	1.8	5	0.93
O(ester)	1.6	7	0.70
O(carbonyl)	1.6	7	0.84
CH <sub>2</sub> or CH <sub>3</sub>	2.0	7	1.77

radii. The constant  $a_{ij}$  was selected to minimize the energy  $E_{ij}$  when  $r_{ij}$  is set equal to the sum of these van der Waals radii for the given pair. The methyl and methylene groups were treated as spherical domains.

Following Brant, *et al.*,<sup>4</sup> coulombic interactions were assessed by assigning partial charges to the atoms using bond moments<sup>5</sup> of 0.74 D for C–O and 2.3 D for C=O. A value of 3.5 was used for the effective dielectric constant.<sup>3</sup> The energy of deformation of the valence angle was estimated according to

$$V(\theta) = A(\Delta\theta)^2 \quad (1)$$

where  $\Delta\theta$  is the distortion of the angle  $\theta$ , and  $A$  is half the force constant. For deformation of  $\angle \text{C}^\alpha \text{CC}^\alpha$  we take  $A = 80$  kcal mol<sup>-1</sup> with  $\Delta\theta$  expressed in radians.<sup>6</sup>

**Geometrical Data.** A portion of an isotactic chain of PMMA is shown in Figure 1, all skeletal bonds being in the trans conformation for which  $\varphi_i = 0$  ( $i = 1$  to  $n$ ). As mentioned in I,<sup>1</sup> the loci of chirality when  $R' \neq R$  are the skeletal bonds and not the so-called asymmetric centers. We adhere to the conventions defined in I regarding  $d$  and  $l$  bonds. In order to distinguish the

(1) P. J. Flory, P. R. Sundararajan, and L. C. DeBolt, *J. Amer. Chem. Soc.*, **96**, 5015 (1974).

(2) A. Abe, R. L. Jernigan, and P. J. Flory, *J. Amer. Chem. Soc.*, **88**, 631 (1966).

(3) P. J. Flory, "Statistical Mechanics of Chain Molecules," Interscience, New York, N. Y., 1969.

(4) D. A. Brant, W. G. Miller, and P. J. Flory, *J. Mol. Biol.*, **23**, 47 (1967).

(5) C. P. Smyth, "Dielectric Behaviour and Structure," McGraw-Hill, New York, N. Y., 1955, p 244.

(6) M. Bixon and S. Lifson, *Tetrahedron*, **23**, 769 (1967).

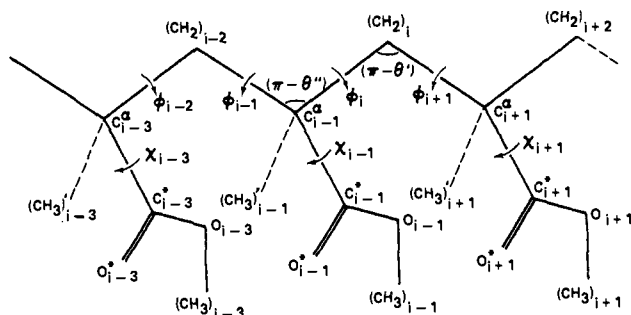


Figure 1. The isotactic PMMA chain.

methyl group attached to  $C^{\alpha}$  from the ester methyl group, we attach a prime to the former, *i.e.*,  $R' = (CH_3)'$ .

The ester group is assumed to be planar with the bond  $O-CH_3$  trans to  $C^{\alpha}-C^*$  and is indicated by an abundance of experimental evidence on various esters.<sup>7</sup> Rotation of the ester group around the  $C^{\alpha}-C^*$  bond is specified by the angle  $\chi$  measured relative to the conformation in which the bond  $C^*=O^*$  is cis to  $C^{\alpha}-CH_3'$ . Infrared spectra of PMMA<sup>8</sup> and of model compounds<sup>9</sup> show the plane of the ester group to be so oriented as to bisect the skeletal bond angle at the  $C^{\alpha}$  atom, the carbonyl bond being either cis or trans to the  $C^{\alpha}-CH_3'$  bond. These alternatives correspond to the conformations  $\chi = 0$  and  $180^\circ$ , respectively. Although steric impingements in the several conformations doubtless induce minor displacements,  $\chi$  is considered below to be restricted to these two values.

The bond lengths and most of the bond angles used in this study, and listed in Table II, were taken from the

Table II. Geometrical Parameters Used for PMMA

Bond	Length, Å	Bond angle	Deg
$C^{\alpha}-CH_2$	1.53	$C-C^{\alpha}-C$	110.0
$C^{\alpha}-CH_3'$	1.53	$C-C^{\alpha}-C^*$	109.5
$C^{\alpha}-C^*$	1.52	$C^{\alpha}-C^*-O$	114.0
$C^*-O$	1.36	$C^*-C^*=O^*$	121.0
$C^*=O^*$	1.22	$C^*-O-CH_3$	113.0
$O-CH_3$	1.45	$C^{\alpha}-C-C^{\alpha}$	122.0

tabulations of Bowen and Sutton.<sup>10</sup> The bond angle  $\angle C^{\alpha}CC^{\alpha}$  at the substituted carbon atom, whose supplement is denoted by  $\theta''$  (see Figure 1), was assigned a value of  $110^\circ$  in recognition of the similarity of the interactions between groups directly attached to  $C^{\alpha}$  and of evidence concerning the corresponding skeletal bond angle in polyisobutylene.<sup>11</sup> With  $\theta''$  thus assigned, energies were calculated as a function of the corresponding angle at the methylene, *i.e.*,  $\theta' = \pi - \angle C^{\alpha}CC^{\alpha}$ , for two skeletal conformations *tt* and *tg*,

(7) L. Pauling and J. Sherman, *J. Chem. Phys.*, **1**, 606 (1933); R. J. B. Marsden and L. E. Sutton, *J. Chem. Soc., London*, 1383 (1936); J. M. O'Gorman, W. Shand, and V. Schomaker, *J. Amer. Chem. Soc.*, **72**, 4222 (1950); J. K. Wilmschurst, *J. Mol. Spectrosc.*, **1**, 201 (1957); R. F. Curl, *J. Chem. Phys.*, **30**, 1529 (1959).

(8) S. Havriliak and N. Roman, *Polymer*, **7**, 387 (1966).

(9) B. Schneider, J. Štokr, S. Dirlikov, and M. Mihailov, *Macromolecules*, **4**, 715 (1971).

(10) H. J. M. Bowen and L. E. Sutton, "Tables of Interatomic Distances and Configurations in Molecules and Ions," Chemical Society, London, 1958; supplement, 1965.

(11) E. Benedetti, C. Pedone, and G. Allegra, *Macromolecules*, **3**, 16, 727 (1970).

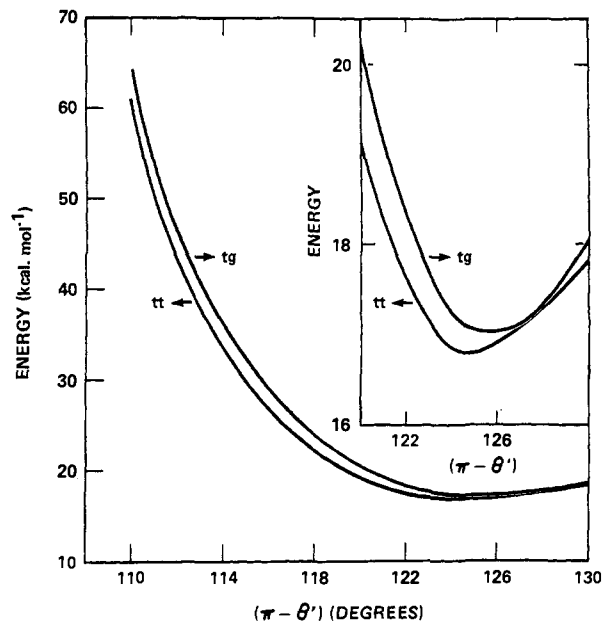
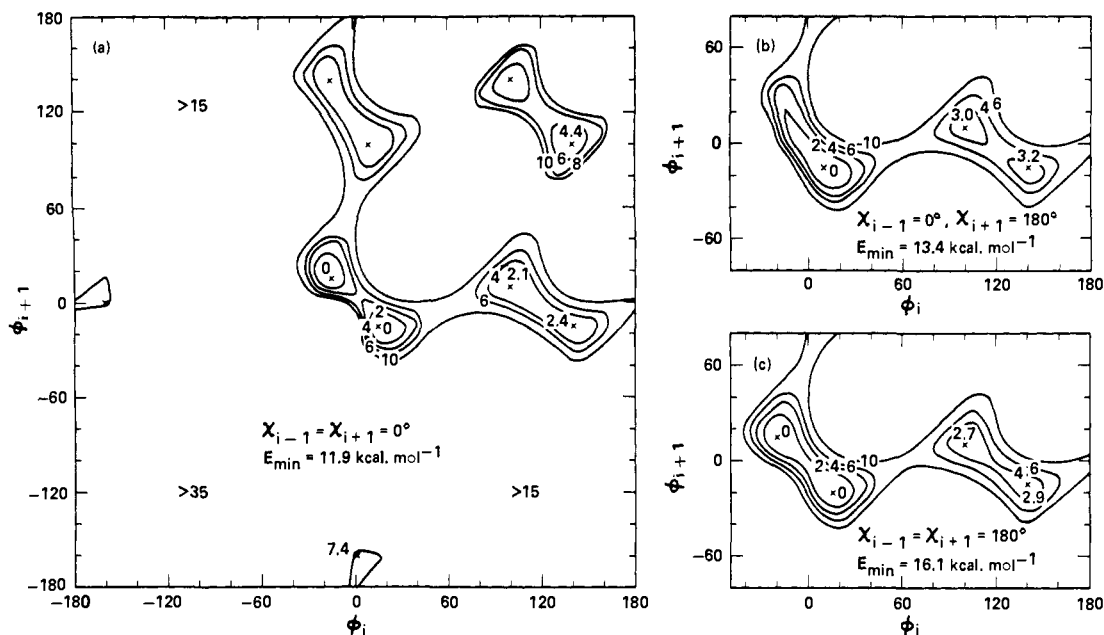


Figure 2. Energies calculated for the *tt* and *tg* conformations of a meso dyad as a function of the skeletal bond angle  $\pi - \theta' = \angle C^{\alpha}CC^{\alpha}$ .

the dyad rotation angles being fixed at their values ( $0$  and  $120^\circ$ ) for perfect staggering. In addition to the angle strain energy given by eq 1, contributions from nonbonded and coulombic interactions were included. Results are presented in Figure 2. For both the *tt* and the *tg* states, the energy decreases rapidly as  $\pi - \theta'$  is increased to *ca.*  $118^\circ$ , then decreases more slowly toward a minimum in the range  $122-126^\circ$ . Thus, the preferred bond angle at the methylene group is indicated to be similar to that for polyisobutylene.<sup>11</sup> A value of  $122^\circ$  was used in the calculations that follow, except where noted otherwise.

**Results of Energy Calculations.** The  $\bar{g}$  conformation invariably imposes severe overlaps between atoms of the ester group and the groups bonded to the adjacent  $C^{\alpha}$  atom. If, for example, bond *i* is  $\bar{g}$ , then for  $\chi_{i-1} = 0^\circ$  the ester oxygen  $O_{i-1}$  overlaps one or the other of the members from the set  $(CH_3)'_{i+1}$ ,  $(CH_2)_{i+2}$ , and  $C^*_{i+1}$ , depending on the rotational state of the bond  $i + 1$ ; the distance between the centers of the overlapping groups is only  $2.1 \text{ \AA}$ . For  $\chi_{i-1} = 180^\circ$ , the distance between one of the above groups and the carbonyl oxygen  $O^*_{i-1}$  is  $2.2 \text{ \AA}$ . These overlaps are excessive for all values of  $\chi_{i-1}$  within the acceptable ranges near  $0$  and  $180^\circ$ . Since the severity of the interactions persists irrespective of the rotations around contiguous skeletal bonds, this may be treated as a first-order interaction.

Conformational energies calculated for a meso dyad are shown in Figure 3 as functions of the rotation angles  $\varphi_i$  and  $\varphi_{i+1}$  (see Figure 1). Contours are shown at intervals of energy quoted in kilocalories per mole relative to the minimum value in each diagram. The energy surface depicted in Figure 3a represents the case in which the adjoining ester substituents are in their preferred orientations:  $\chi_{i-1} = \chi_{i+1} = 0^\circ$ . The complete ranges of the rotation angles are covered in this diagram. Figures 3b and 3c present corresponding calculations within the more important ranges of  $\varphi_i$  and  $\varphi_{i+1}$  for the ester group orientations  $\chi_{i-1} = 0^\circ$ ,  $\chi_{i+1} = 180^\circ$ , and  $\chi_{i-1} = \chi_{i+1} = 180^\circ$ , respectively. Energies used for



**Figure 3.** Energies calculated for a meso dyad as a function of skeletal bond rotations  $\varphi_i$  and  $\varphi_{i+1}$  for the ester group orientations denoted by  $\chi_{i-1}$  and  $\chi_{i+1}$  in each diagram. Locations of minima are denoted by X. Energy contours are labeled in kilocalories per mole relative to the lowest minimum, labeled 0. They have been interpolated from energies calculated at intervals of 5 or 20° in  $\varphi_i$  and  $\varphi_{i+1}$ , as explained in the text. "Absolute" energies  $E_{\min}$  at the lowest minima (tt) are given in each diagram. Rotation angles are reckoned in the senses specified in I; <sup>1</sup> i.e., for the meso dyad represented as *dl* in Figure 1,  $\varphi_i$  and  $\varphi_{i+1}$  are measured in the right- and left-handed senses, respectively.

construction of the contours in Figure 3 were calculated at intervals of 5° in  $\varphi_i$  and  $\varphi_{i+1}$  within ranges of  $\pm 40^\circ$  of the positions for perfect staggering ( $0^\circ$ ,  $\pm 120^\circ$ ). Outside these ranges intervals of 20° were employed. Expanded plots of contours for the energy surfaces of Figure 3a in the vicinities of the tt and gt states are shown in Figure 4. Energy contours shown in Figures 3 and 4 were located by interpolation.

The "absolute" conformational energies at the lowest minima in each of the three diagrams in Figure 3 are  $E_{\min} = 11.9$ , 13.4, and 16.1 kcal mol<sup>-1</sup>, respectively. The larger values in Figures 3b and 3c are due primarily to the difference between  $\angle C^\alpha C^* O^*$  and  $\angle C^\alpha C^* O$ , the former exceeding the latter by 7°; see Table II. The orientation  $\chi = 0^\circ$  places  $O_{i-1}^*$  at a distance of 2.7 Å from  $(CH_3)_{i-1}'$ ; for  $\chi = 180^\circ$ ,  $O_{i-1}$  is 2.6 Å from  $(CH_3)_{i-1}'$ . Consequently,  $E_{\min}$  in Figure 3b exceeds  $E_{\min}$  in Figure 3a by 1.5 kcal mol<sup>-1</sup>; the difference is nearly three times as great in Figure 3c where both  $\chi_{i-1}$  and  $\chi_{i+1}$  are 180°.

The high energies for all conformations near  $\varphi_i = -120^\circ$  or  $\varphi_{i+1} = -120^\circ$  confirm the virtual inaccessibility of the  $\bar{g}$  regions indicated by the intergroup distances cited above. The minima near  $(0^\circ, -160^\circ)$  and  $(-160^\circ, 0^\circ)$  are of no consequence because of their high energies (7.4 kcal mol<sup>-1</sup>) and the confinement of their domains to small regions.

For  $\chi_{i-1} = \chi_{i+1} = 0$  and 180° (see Figures 3a, 3c, and 4), pairs of minima occur in the vicinity of each admissible staggered conformation, namely, tt, tg, gt, and gg. According to the calculations carried out at intervals of 5°, these are located at displacements  $\Delta\varphi_i$  and  $\Delta\varphi_{i+1}$  of about  $\pm 15$  and  $\mp 15^\circ$  from the angles at 120° intervals for perfect staggering of tetrahedrally bonded atoms. This feature of the conformational energy surface finds explanation in the partial alleviation of the severe second-order steric repulsions, prevalent in all

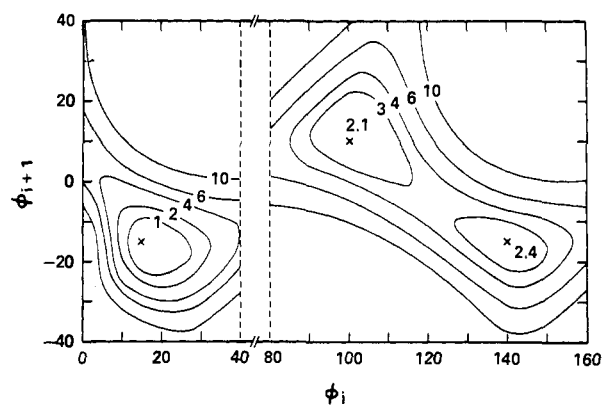


**Figure 4.** Conformational energies shown in enlarged scale for the meso dyad with  $\chi_{i-1} = \chi_{i+1} = 0^\circ$  in the vicinities of the tt and gt states in Figure 3a. See legend for Figure 3.

staggered conformations, through coordinated adjustments in  $\varphi_i$  and  $\varphi_{i+1}$ . These adjustments must be of opposite *sign* for the respective rotation angles, the conventions on signs of rotation set forth in I being followed. (They correspond to rotations which are of the same *sense*, i.e., both right-handed or both left-handed, in the case of a meso dyad, one skeletal bond of which is *d* and the other *l* according to the definitions introduced in I.) In the staggered conformation  $(\varphi_i, \varphi_{i+1}) = (0^\circ, 0^\circ)$ ; for example, both of the distances  $(CH_3)_{i-1}' \cdots (CH_3)_{i+1}'$  and  $C^*_{i-1} \cdots C^*_{i+1}$  are 2.8 Å, which is about 1.2 Å less than the sum of the van der Waals radii for the methyl groups. Overlaps also occur between  $O_{i-1}$  and  $O_{i+1}$  (2.7 Å) and between the substituents  $(CH_3)_{i-1}$  and  $(CH_3)_{i+1}$  (2.9 Å). For  $\Delta\varphi$ 's of  $\pm 15^\circ$  the two former distances are increased to *ca.* 3.1 Å and the  $O_{i-1} \cdots O_{i+1}$  and  $(CH_3)_{i-1} \cdots (CH_3)_{i+1}$  distances to 3.1 and 3.7 Å, respectively. Displacements  $\Delta\varphi$  of the same sign

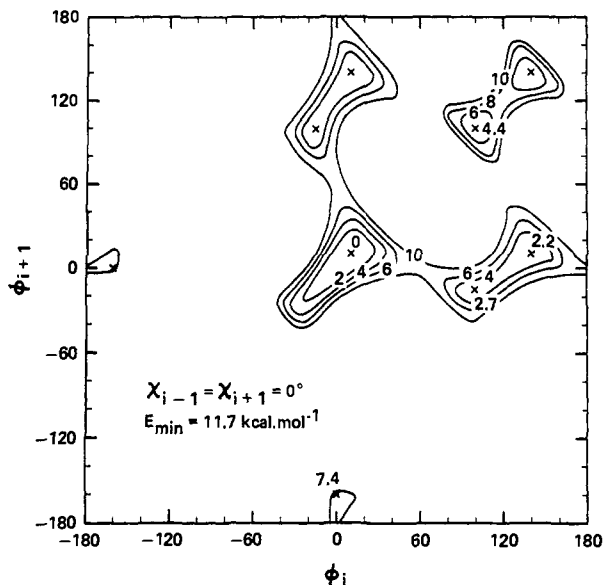


**Figure 5.** Energies calculated for a *dd* racemic dyad with  $\chi_{i-1} = \chi_{i+1} = 0^\circ$ . See legend for Figure 3. Rotation angles are reckoned in the sense specified in I; *i.e.*, for the *dd* racemic dyad  $\varphi_i$  and  $\varphi_{i+1}$  are measured in the right-handed sense.

diminish the distances between the several interacting pairs and hence are strongly disfavored.

Displacements  $|\Delta\varphi|$  appreciably greater than  $20^\circ$  are opposed by "diagonal interactions" between groups on opposite sides of the plane defined by the skeletal bonds  $i$  and  $i+1$ . In the vicinity of the *tt* conformation the groups involved are  $(\text{COOCH}_3)_{i-1}$  and  $(\text{CH}_3)_{i+1}$  or  $(\text{CH}_3)_{i-1}$  and  $(\text{COOCH}_3)_{i+1}$ ; the distances  $\text{C}^*_{i-1} \cdots (\text{CH}_3)_{i+1}$  and  $(\text{CH}_3)_{i-1} \cdots \text{C}^*_{i+1}$  are  $3.8 \text{ \AA}$  for  $(\varphi_i, \varphi_{i+1}) = (0^\circ, 0^\circ)$ . For  $(-15^\circ, 15^\circ)$ , the former decreases to  $3.1 \text{ \AA}$ ;  $(\text{CH}_3)_{i-1} \cdots \text{C}^*_{i+1}$  is lowered to  $3.1 \text{ \AA}$  by the opposite displacement  $(15^\circ, -15^\circ)$ . The further decrease of one of these with increase in the magnitude of the displacements  $|\Delta\varphi|$  accounts for the steep rise in the energy for  $|\Delta\varphi| > 30^\circ$ .

The character of the pair of diagonal interactions, and especially their symmetry, for each conformational domain is reflected in the pair of minima and in the form of the surface surrounding them. Thus, because of the equivalence of the interactions for  $(+, -)$  and for  $(-, +)$ , displacements in the neighborhood of the *tt* conformation when  $\chi_{i-1} = \chi_{i+1}$  as in Figures 3a and 3c, the energy surface is symmetric with respect to the line  $\varphi_{i+1} = \varphi_i$ , and the two minima of the pair are of equal energy. Analogous symmetry relative to the bisecting diagonal line holds in the *gg* region.

The energy surface is unsymmetric in the *gt* and *tg* domains. This follows from the fact that the diagonal interactions for *gt* involve  $(\text{CH}_3)_{i-1}$  with  $(\text{CH}_3)_{i+1}$  for the  $(-, +)$  displacement and  $(\text{CH}_2)_{i-2}$  with the  $\text{C}^*$  and  $\text{O}^*$  atoms of  $(\text{COOCH}_3)_{i+1}$  for  $(+, -)$ , the ester groups being in the same orientation, *i.e.*, for  $\chi_{i-1} = \chi_{i+1}$  as in Figures 3a and 3c. The opposite holds for *tg*. The evident asymmetry of these domains in Figure 3a notwithstanding, the energies at the two minima happen to be about the same at the level of refinement of these calculations. (The foregoing identifications of order of  $+$  and  $-$  signs holds for the "*d*" meso dyad displayed in Figure 1. Reversal of the diagram so that

the dyads read "*ld*" obviously would necessitate reversal in the order of  $+$  and  $-$ .)

When  $\chi_{i-1}$  and  $\chi_{i+1}$  are assigned different values as in Figure 3b, the symmetry of the  $(+, -)$  and  $(-, +)$  displacements from *tt* is destroyed. The former displacement is preferred over the latter to the extent that only the former minimum remains. This is a consequence of the juxtaposition of ester groups, in opposite orientations, these groups being quite unsymmetric about the  $\text{C}^\alpha\text{-C}^*$  axis.

The energy at the saddle between the *tt* pair is much lower in Figure 3c than in 3a, but this difference is of little significance. The differences between the "absolute" energies in Figures 3a, 3b, and 3c are of foremost importance. The zero of energy for the  $\chi_{i-1} = \chi_{i+1} = 180^\circ$  diagram (Figure 3c) is  $4.2 \text{ kcal mol}^{-1}$  above that for  $\chi_{i-1} = \chi_{i+1} = 0^\circ$  (Figure 3a). This difference is sufficient to render the  $(180^\circ, 180^\circ)$  configuration of negligible significance in the analysis of the configurational statistics. When the side-chain configuration is  $\chi_{i-1} = 0^\circ$ ,  $\chi_{i+1} = 180^\circ$  (Figure 3b), or equivalently  $\chi_{i-1} = 180^\circ$ ,  $\chi_{i+1} = 0^\circ$ , the energy at the *tt* minimum is raised by *ca.*  $1.5 \text{ kcal mol}^{-1}$  compared to the *tt* minima for  $\chi_{i-1} = \chi_{i+1} = 0$ . Hence, the former side-chain orientations (Figure 3b) should contribute to some extent. The inclusion of these less favorable side-chain orientations is free of complications because of the similarities of the surfaces to that in Figure 3a.

In view of the approximate two-fold symmetry of the regions of the surface surrounding each principal domain, the *tt* state in Figure 3b excepted, approximation of each region by a single state located very near the position for perfect staggering should be legitimate.<sup>12</sup> In support of this conjecture,  $\varphi_i$  and  $\varphi_{i+1}$  were averaged over each domain, values of the angles at  $5^\circ$  intervals being weighted by Boltzmann factors of the energy calculated at each point. The resulting average displacements in  $\varphi_i$  and  $\varphi_{i+1}$  did not exceed  $4^\circ$  in any instance, with the exception noted above; the departure of this conformation from  $(0^\circ, 0^\circ)$  is unimportant owing to its small statistical weight. Hence, with an error doubtless of less consequence than uncertainties in the energies, it is permissible to represent each domain by a single state located at the position 0 or  $120^\circ$ , for perfect staggering.

The conformational energy surface analogous to Figure 3a but for a racemic dyad is shown in Figure 5. It was obtained by calculating energies at intervals in  $\varphi_i$  and  $\varphi_{i+1}$  of  $5^\circ$  in the regions of the minima and at intervals of  $20^\circ$  elsewhere, exactly as for the meso dyad (Figures 3 and 4). The only significant difference compared to Figure 3a occurs in the form of the surface in the vicinity of the *tt* state, where the racemic dyad displays a single minimum.

### Statistical Weights

Exclusion of the  $\bar{g}$  state for the skeletal bonds obviates the need to consider the interactions of fourth order treated in I, since each such conformation includes two  $\bar{g}$  states among the sequence of four bonds. The larger statistical weight matrices that embrace sets of four bonds are therefore unnecessary for the treatment of PMMA. Instead, the matrices  $\mathbf{U}'$  and  $\mathbf{U}''$  for bond pairs suffice, and with the exclusion of the

(12) P. J. Flory, *J. Polym. Sci., Part A-2*, 11, 621 (1973).

$\bar{g}$  state these matrices reduce to  $2 \times 2$  order. From eq 8, 13, and 14 in I, we thus obtain, after normalization of the  $U''$  matrices

$$U' = \begin{bmatrix} 1 & 1 \\ 1 & 0 \end{bmatrix} \quad (2)$$

$$U_m'' = \begin{bmatrix} 1 & \alpha \\ \alpha & \alpha^2/\beta \end{bmatrix} \quad (3)$$

$$U_r'' = \begin{bmatrix} \beta & \alpha \\ \alpha & \alpha^2/\beta \end{bmatrix} \quad (4)$$

where  $\alpha$  and  $\beta$  are defined by eq 11 and 12 in I.

Partition functions  $z_{tt}$ ,  $z_{gt}$ , etc., for the various minima for both meso and racemic dyads were calculated by taking the sums of Boltzmann factors of the energy at  $5^\circ$  intervals over the respective domains. Energies were taken relative to the minima for the tt state of the meso dyad in each instance. A temperature of  $300^\circ\text{K}$  was chosen. Results of these calculations are given in the second column of Table III.

**Table III.** Parameters Deduced from the Energy Calculations ( $T = 300^\circ\text{K}$ )

	$z_s^a$	$z_s/z_{tt,m}$	$\langle E \rangle_s^b$ , cal mol $^{-1}$
tt, meso	11.79	1.0	0
gt, meso	0.43	0.04	2200
gg, meso	0.01	0.001	4500
tt, racemic	19.23	1.63	100

<sup>a</sup> Expressed as the sum over  $5^\circ$  intervals; see text. <sup>b</sup> Relative to tt, meso.

The ratios  $z_s/z_{tt,m}$  of the statistical weights  $z_s$  for the several states expressed relative to the statistical weight for the tt state of the meso dyad (see eq 2-4) are recorded in the third column. Average energies appearing in the last column were calculated according to

$$\langle E_s \rangle = z_s^{-1} \sum_{\varphi_i, \varphi_{i+1}} E_{\varphi_i, \varphi_{i+1}} \exp(-E_{\varphi_i, \varphi_{i+1}}/RT) \quad (5)$$

These calculations, like those presented above, were carried out by summation at  $5^\circ$  intervals with  $T = 300^\circ\text{K}$ .

We let

$$\alpha = \alpha_0 \exp(-E_\alpha/RT) \quad (6)$$

where  $E_\alpha = \langle E_{gt,m} \rangle - \langle E_{tt,m} \rangle$ . Since, according to eq 3,  $\alpha = z_{gt,m}/z_{tt,m}$  we have from the results in Table III

$$\alpha = 1.6 \exp(-2200/RT) \quad (7)$$

where  $R$  is in cal mol $^{-1}$  deg $^{-1}$ . Similarly, letting

$$\beta = \beta_0 \exp(-E_\beta/RT) \quad (8)$$

where  $E_\beta = \langle E_{tt,r} \rangle - \langle E_{tt,m} \rangle$  and  $\beta = z_{tt,r}/z_{tt,m}$  according to eq 3 and 4, we obtain

$$\beta = 1.4 \exp(100/RT) \quad (9)$$

Departures of  $\alpha_0$  and  $\beta_0$  from unity reflect the dissimilarities in the shapes of the gt, meso and tt, racemic minima compared to that for tt, meso; see Figures 3-5.

The results are regarded as estimates in recognition of the limitations of the conformational energies.

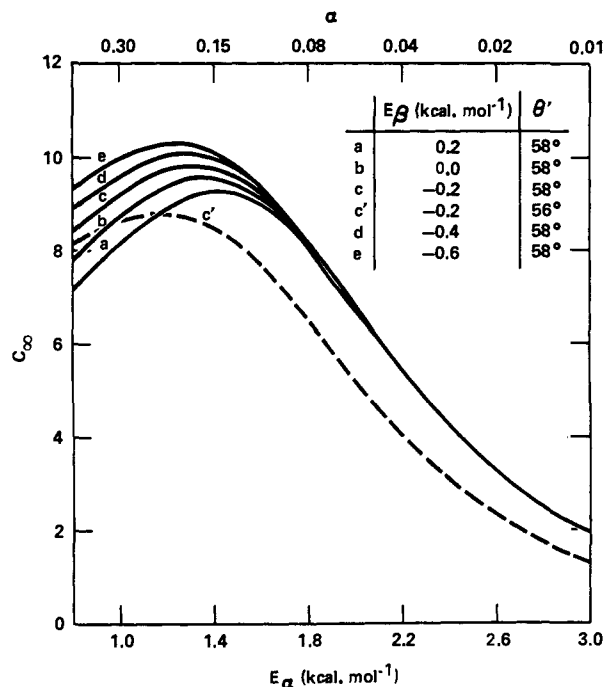


**Figure 6.** Dependence of  $C_\infty$  on  $E_\alpha$  and  $E_\beta$  for isotactic PMMA with  $\theta' = 58^\circ$  (solid curves) and  $\theta' = 56^\circ$  (broken curve);  $T = 300^\circ\text{K}$ .

The shapes of the minima, however, are comparatively insensitive to the values of parameters adopted for the calculations, *i.e.*, to the values chosen for  $\theta'$  and for the van der Waals radii of atoms and groups. On the other hand, values calculated for the energies are subject to appreciable uncertainty, depending upon choices of parameters. Accordingly, in the calculations that follow  $\alpha_0$  and  $\beta_0$  were fixed, and adjustments were made in  $E_\alpha$  and  $E_\beta$ .

### Characteristic Ratios

**Isotactic Chains.** Characteristic ratios  $C_n = \langle r^2 \rangle_0/nl^2$  were calculated according to established methods described previously.<sup>3,13,14</sup> Figure 6 shows the dependence of  $C_\infty = \lim_{n \rightarrow \infty} C_n$  for isotactic (meso) PMMA on  $E_\alpha$  for several values of  $E_\beta$ . The skeletal angle at  $\text{CH}_2$  was fixed at  $\theta' = 58^\circ$  and a temperature of  $300^\circ\text{K}$  was used throughout.

As  $\alpha$  is reduced toward zero, gauche states are suppressed and the chain is forced into the planar, all-trans conformation. Since  $\theta' \neq \theta''$ , the form of the chain in the limit  $\alpha = 0$  is polygonal.<sup>3,15</sup> With an increase in  $\alpha$ , sequences of units in compact planar conformations are disrupted by the occurrence of gauche bonds. Hence,  $C_\infty$  increases with  $\alpha$ , reaching a maximum at  $\alpha \approx 0.21$ . It decreases with further increase in  $\alpha$  owing to disordering by interspersions of numerous gauche conformations. In the range of  $\alpha \sim < 0.13$  ( $E_\alpha > 1.5$  kcal mol $^{-1}$ ), a positive temperature coefficient is implied.

For the meso chain, the value of  $\beta$  is significant only for values of  $\alpha$  sufficiently great to yield gauche conformers in substantial abundance. This follows from

(13) P. J. Flory, J. E. Mark, and A. Abe, *J. Amer. Chem. Soc.*, **88**, 639 (1966).

(14) Y. Fujiwara and P. J. Flory, *Macromolecules*, **3**, 280 (1970).

(15) P. J. Flory, V. Crescenzi, and J. E. Mark, *J. Amer. Chem. Soc.*, **86**, 146 (1964).

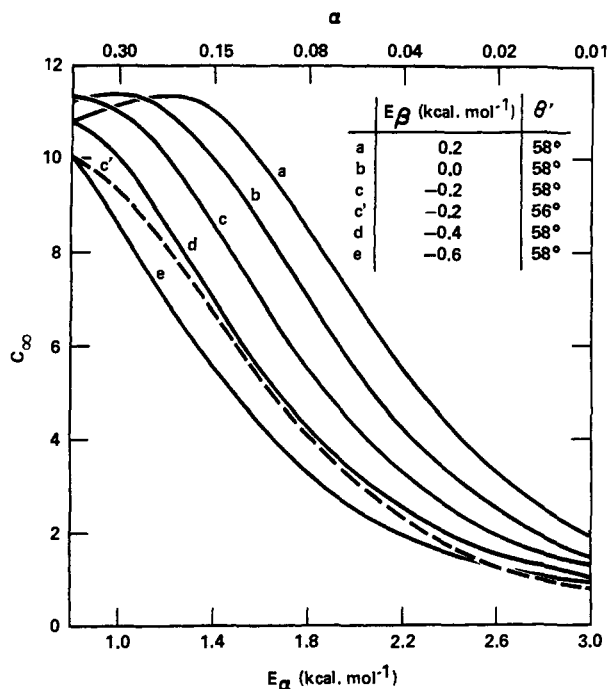


Figure 7. Dependence of  $C_\infty$  on  $E_\alpha$  and  $E_\beta$  for syndiotactic PMMA with  $\theta' = 58^\circ$  (solid curves) and  $\theta' = 56^\circ$  (broken curve);  $T = 300^\circ\text{K}$ .

the form of  $U''$  (see eq 3) which specifies the role of  $\beta$  as influencing, inversely, the incidence of gg conformations. Depletion of these conformations raises  $C_\infty$ , as should be expected.

If  $E_\alpha$  and  $E_\beta$  are assigned the values 2.2 and  $-0.1$  kcal mol<sup>-1</sup>, respectively, as indicated by the energy calculations above, then  $C_\infty = 5.5$ . This is well below the indications of experimental results which fall in the range 9.2–10.7<sup>16,17</sup> for predominantly isotactic chains. In order to reproduce the latter,  $E_\alpha$  must be reduced to about  $1.2 \pm 0.4$  kcal mol<sup>-1</sup>. The alteration probably is within the limits of reliability of the semiempirical energy calculations. If bond angles were allowed to vary with conformation as required to minimize the energy, then the calculated value of  $E_\alpha$  would certainly be lowered. The adjustment in  $E_\alpha$  is in the direction to be expected on this basis.

**Syndiotactic Chains.** Corresponding calculations for syndiotactic (racemic) PMMA are presented in Figure 7. The parameter  $\beta$  plays a more prominent role in this case, as is indicated in eq 4; the factor  $\alpha$  weights the gauche states, exactly as for the meso chain. The dependence of  $C_\infty$  on  $\alpha$  resembles that for the isotactic chain and for the same reasons; *i.e.*, closure of planar sequences is the overriding feature when the population of gauche conformations is low. As  $\beta$  is increased (*i.e.*, as  $E_\beta$  is decreased),  $C_\infty$  is lowered owing to the increase in trans states, and these conduce to compactness of conformation as pointed out above.

Experiments indicate  $C_\infty = 7.3$ –8.4 for predominantly syndiotactic chains.<sup>16,17</sup> This range is reproduced by  $E_\alpha = 1.6$  to 1.75 kcal mol<sup>-1</sup> and  $E_\beta = 0$ , values that are fairly close to those indicated by the conforma-

(16) I. Sakurada, A. Nakajima, O. Yoshizaki, and K. Nakamae, *Kolloid-Z.*, **186**, 41 (1962).

(17) G. V. Schulz and R. Kirste, *Z. Phys. Chem. (Frankfurt am Main)*, **30**, 171 (1961); G. V. Schulz, W. Wunderlich, and R. Kirste, *Makromol. Chem.*, **75**, 22 (1964).

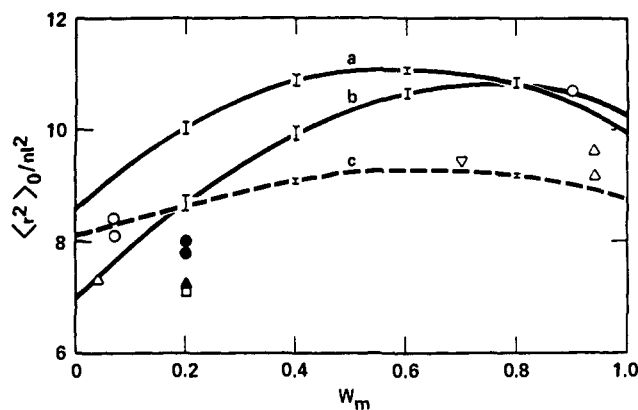


Figure 8. Characteristic ratios calculated for Monte Carlo chains of 200 units each. Standard deviations are marked by vertical bars. Curves shown are for (a)  $E_\alpha = 1.0$ ,  $E_\beta = -0.6$ , and  $\theta' = 58^\circ$ ; (b)  $E_\alpha = 1.2$ ,  $E_\beta = -0.6$ , and  $\theta' = 58^\circ$ ; (c)  $E_\alpha = 1.2$ ,  $E_\beta = -0.2$ , and  $\theta' = 56^\circ$ , energies being in kilocalories per mole. The experimental results of various authors are represented by points as follows: ( $\odot$ ) Sakurada, *et al.*,<sup>16</sup> ( $\Delta$ ) Schulz, *et al.*,<sup>17</sup> ( $\nabla$ ) Krause and Cohn-Ginsberg,<sup>19</sup> ( $\bullet$ ) Chinai and Valles,<sup>20</sup> ( $\blacktriangle$ ) Fox,<sup>21</sup> and ( $\square$ ) Vasudevan and Santappa.<sup>22</sup>

tional energy calculations. The experimental results are satisfied alternatively by taking  $E_\alpha = 1.0$  to 1.15 kcal mol<sup>-1</sup> and  $E_\beta = -0.6$  kcal mol<sup>-1</sup>. These values are consistent also with the results for isotactic chains.

**Stereoirregular Chains.** Monte Carlo methods were employed to generate chains consisting of 200 units with random sequencing of meso and racemic dyads; *i.e.*, the Monte Carlo generation of chains was conducted according to Bernoullian statistics. The expectation  $w_m$  of meso placement was varied in increments of 0.2 between 0 and 1. Averages of the characteristic ratios calculated for sets of five such chains are plotted against  $w_m$  in Figure 8 for the values of  $E_\alpha$  and  $E_\beta$  quoted therein. Standard deviations within sets are indicated by vertical bars. The curves are convex rather than concave as found for monosubstituted vinyl chains.<sup>3,14,18</sup> In the latter, the characteristic ratio for either stereoregular polymer ( $w_m = 0$  or 1.0) is reduced by a minor proportion of the unit of opposite stereoisomeric character.<sup>3,18</sup> The curves calculated for PMMA (Figure 8) show  $C_\infty$  to increase slightly with stereoirregularity at the extremities, contrary to precedent for monosubstituted vinyl chains. The enhancement of the dimensions by stereoirregularity in PMMA is comparatively small, however.

Included in Figure 8 are experimental results from various sources as noted in the legend. In instances where the tacticities have been quoted by the authors,<sup>16,17</sup> their values have been adopted in assigning  $w_m$ . In other cases,<sup>19–22</sup> values of  $w_m$  have been taken from the work of Bovey<sup>23</sup> for PMMA's prepared at a comparable temperature using the same type of initiation. These data gathered from diverse sources are insufficiently consistent and complete for a definitive

(18) A. Tonelli, Ph.D. Thesis, Stanford University, 1968.

(19) S. Krause and E. Cohn-Ginsberg, *J. Phys. Chem.*, **67**, 1479 (1963).

(20) S. N. Chinai and R. J. Valles, *J. Polym. Sci.*, **39**, 363 (1959).

(21) T. G. Fox, *Polymer*, **3**, 111 (1962).

(22) P. Vasudevan and M. Santappa, *J. Polym. Sci., Part A-2*, **9**, 483 (1971).

(23) F. A. Bovey and G. V. D. Tiers, *J. Polym. Sci.*, **44**, 173 (1960); F. A. Bovey, *Accounts Chem. Res.*, **1**, 175 (1968); F. A. Bovey, *J. Polym. Sci.*, **46**, 59 (1960).

test of the foregoing predictions concerning the dependence of the characteristic ratio on tacticity. However, the results of Krause and Cohn-Ginsberg,<sup>19</sup> which include one point in the intermediate range, do indeed suggest qualitative conformity with theory. Thus,  $C_\infty$  is roughly independent of  $w_m$  from 1 to 0.7 according to their results; it decreases somewhat from  $w_m = 0.7$  to 0.04. The absence of a minimum is indicated, and this is in agreement with our calculations.

**The Temperature Coefficient of  $\langle r^2 \rangle_0$ .** Calculated values of  $d \ln C_\infty / dT = d \ln \langle r^2 \rangle_0 / dT$  are plotted in Figure 9 against  $E_\alpha$  for isotactic and syndiotactic PMMA chains for the values of  $E_\beta$  indicated. For the former, the temperature coefficient is negative throughout the range  $E_\alpha = 0.8$  to 1.5 kcal mol<sup>-1</sup> found to be required for agreement with experimental results on the characteristic ratio.

The temperature coefficient for the syndiotactic chain depends strongly on  $E_\beta$ , as well as on  $E_\alpha$ . For  $E_\beta = 0$  and  $E_\alpha < 1.1$  kcal mol<sup>-1</sup> it is negative, though very small. For  $E_\beta = -0.6$  kcal mol<sup>-1</sup> it is positive and rises steeply with  $E_\alpha$ . Thus, the temperature coefficients for isotactic and syndiotactic chains may differ markedly, this being in contrast to the similarity in the magnitudes of  $C_\infty$  for the two stereoregular PMMA chains. Moreover, the temperature coefficients are sensitive to small changes in the energies  $E_\alpha$  and  $E_\beta$ , within certain ranges of these energies at any rate.

Experimental evidence on the temperature coefficient of  $C_\infty$  is indecisive.<sup>24</sup> Fox<sup>21</sup> reported a value of zero for conventional PMMA (ca. 80% syndiotactic). The work of Vasudevan and Santappa<sup>22</sup> indicated no definite dependence of  $C_\infty$  on temperature. The results of Sakurada, *et al.*,<sup>16</sup> on syndiotactic PMMA give  $d \ln C_\infty / dT = 1.4 \times 10^{-3}$  K<sup>-1</sup>. Positive values have been reported also by Schulz and Kirste<sup>17</sup> ( $2.4 \times 10^{-3}$  K<sup>-1</sup>) and by Moore and Fort<sup>25</sup> ( $4.0 \times 10^{-3}$  K<sup>-1</sup>). For isotactic PMMA, Sakurada, *et al.*,<sup>16</sup> found a negative temperature coefficient,  $d \ln C_\infty / dT = -2.3 \times 10^{-3}$  K<sup>-1</sup>.

(24) U. Bianchi, *J. Polym. Sci., Part A*, **2**, 3083 (1964).

(25) W. R. Moore and R. F. Fort, *J. Polym. Sci., Part A*, **1**, 929 (1963).

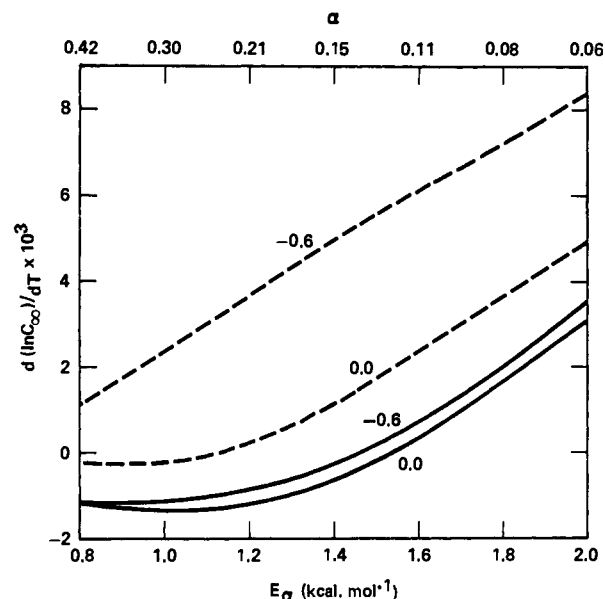


**Figure 9.** Dependence of  $d \ln C_\infty / dT$  on  $E_\alpha$  and  $E_\beta$  for isotactic (solid curves) and syndiotactic (broken curves) PMMA, with  $\theta' = 58^\circ$ . Values of  $E_\beta$  in kilocalories per mole are given on the curves;  $T = 300^\circ\text{K}$ .

All of these results were obtained from intrinsic viscosities without adequate measures to eliminate specific effects of the solvents.<sup>26</sup> The more reliable method of determination of  $d \ln C_\infty / dT$  from the temperature coefficient of stress exhibited by a strained network has not been applied to PMMA. According to such evidence as is available,  $d \ln C_\infty / dT$  may be positive and fairly large for the predominantly syndiotactic polymer and negative for the isotactic PMMA. These results are in qualitative accord with calculations using a consistent set of parameters for all data, e.g., using  $E_\alpha \approx 1.1$  and  $E_\beta \approx -0.6$  kcal mol<sup>-1</sup>.

**Acknowledgment.** This work was supported by the Directorate of Chemical Sciences, U. S. Air Force Office of Scientific Research Grant No. 73-2441A.

(26) J. E. Mark, *Rubber Chem. Technol.*, **46**, 593 (1973).